JACS
JOURNAL OF THE AMERICAN CHEMICAL SOCIETY
Article
pubs.acs.org/JACS

Mechanistic Insights into the BINOL-Derived Phosphoric Acid-Catalyzed Asymmetric Allylboration of Aldehydes

Matthew N. Grayson,[†] Silvina C. Pellegrinet,[‡] and Jonathan M. Goodman*[,†]

[†]Unilever Centre for Molecular Science Informatics, Department of Chemistry, University of Cambridge, Lensfield Road, Cambridge CB2 1EW, United Kingdom

[‡]Instituto de Química Rosario (CONICET), Facultad de Ciencias Bioquímicas y Farmacéuticas, Universidad Nacional de Rosario, Suipacha 531, Rosario (2000), Argentina

Supporting Information

ABSTRACT: BINOL-derived phosphoric acids catalyze the asymmetric allylboration of aldehydes. DFT and QM/MM hybrid calculations showed that the reaction proceeds via a transition state involving both a hydrogen-bonding interaction from the catalyst hydroxyl group to the pseudoaxial oxygen of the cyclic boronate and a stabilizing interaction from the phosphoryl oxygen of the catalyst to the formyl hydrogen of the aldehyde. These interactions lower the energy of the transition structure and provide extra rigidity to the system. This mechanistic pathway is consistent with the experimentally observed enantioselectivity except in one case. We have used our model's predictions to guide our own experimental work. The conflict is resolved in favor of our calculations.

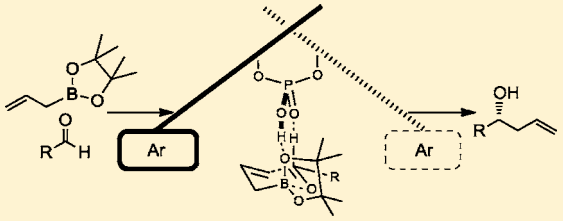

1. INTRODUCTION

Allylboration has become an important reaction for the stereoselective formation of carbon−carbon bonds.[1,2] These reactions proceed via cyclic, six-membered ring chairlike transition states (TSs) involving the activation of the carbonyl by the boron atom.[3,4] As a result, they are highly stereoselective. Brown developed highly enantioselective allylboration reactions using pinene-derived reagents,[5,6] and more recently catalytic methods have emerged such as work by Hall[7] and Shibasaki.[8]

In 2010, Antilla et al. reported the use of a chiral BINOL-derived phosphoric acid as an efficient catalyst for the allylboration of aldehydes, which gave the corresponding homoallylic alcohols in excellent yields and enantioselectivities (Scheme 1).[9] However, it is not altogether clear how the chiral catalyst induces such strong enantioselectivity. Antilla suggested a six-membered ring chairlike transition state with activation of the pseudoequatorial oxygen of the cyclic boronate via protonation by the chiral phosphoric acid catalyst to explain the reactivity (Antilla's model, Scheme 1). Such a model, in which the catalyst binds to the reactants through its Brønsted acidic site only, seems too flexible to account for the high experimental enantiomeric ratios. Furthermore, our previous investigations into similar BINOL-derived phosphoric acid-catalyzed reactions have shown that single-point binding from the catalyst to the substrate cannot explain the observed enantioselectivity, whereas double coordination from both the P═O and the P−O−H groups leads to good enantioselectivity.[10,11]

Herein, we report the results of DFT and QM/MM hybrid calculations, which suggest that the reaction involves both a hydrogen-bonding interaction from the catalyst hydroxyl group to the pseudoaxial oxygen of the cyclic boronate and a stabilizing interaction from the phosphoryl oxygen of the catalyst to the formyl hydrogen of the aldehyde. These interactions lower the energy of the transition structure and provide extra rigidity to the system.

Scheme 1. Asymmetric Allylboration of Aldehydes[9]

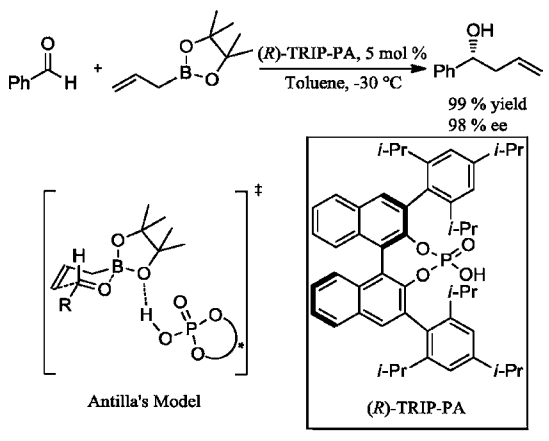

2. COMPUTATIONAL DETAILS

To gain mechanistic insight into the origins of the enantioselectivity observed in the BINOL-derived phosphoric acid-catalyzed allylboration of aldehydes, we performed a thorough theoretical study using three different approaches.

The preferred reaction pathway was first investigated using buta-1,3-diene-1,4-diol-phosphoric acid as a model for the catalyst,[11] before

Received: October 30, 2011
Published: January 2, 2012

dx.doi.org/10.1021/ja210200d | J. Am. Chem.Soc. 2012, 134, 2716−2722

studying the full molecular system. Quantum mechanical calculations were performed using the Jaguar program (version 7.6).[12] The B3LYP density functional,[13,14] and split-valence polarized 6-31G** basis set,[15,16] were used for all geometry optimizations. Single-point energies were taken using the M06-2X density functional[17] and 6-31G** basis set.[15,16] This energy was used to correct the gas-phase energy obtained from the B3LYP calculations.[18] Activation free energies are quoted relative to infinitely separated reagents.

To further validate the results obtained with the model system, we also performed full B3LYP/6-31G* calculations using the phosphoric acid derived from (*R*)-3,3′-bis(2,4,6-trimethylphenyl)-1,1′-bi-2-phenol as a model,[19] implemented in Gaussian 03 (revision C.02).[20]

For the QM/MM hybrid calculations on the full catalyst, transition states were located using the ONIOM method implemented in Gaussian 03 (revision E.01).[20] B3LYP/6-31G** was used for the high-layer, and the force field UFF[21] was used for the low-layer. The reactants and the phosphoric acid moiety of the catalyst were included in the high-layer, and the remaining regions of the catalyst were treated as the low-layer. The combination of DFT and UFF has previously been shown to give excellent results when used to describe reactions catalyzed by chiral phosphoric acids.[10,22] The position of the partition within the catalyst was chosen as the phosphoric acid binds directly to the reagents, whereas the rest of the catalyst acts as steric bulk and can be adequately described by molecular mechanics.[10] M06-2X/6-31G** single-point energy calculations were performed on the resulting structures using the Jaguar program (version 7.6) and used to correct the gas-phase energy derived from the ONIOM calculations.[18]

Free energies in solution were derived from structures optimized in the gas phase at the B3LYP/6-31G** level of theory by means of a single-point calculation using M06-2X/6-31G** with the polarizable continuum model (PCM) as implemented in the Jaguar program (version 7.6) using toluene (probe radius = 2.76 Å) as the solvent.[23] These values were used to correct the Gibbs free energy derived from the ONIOM calculations.

3. RESULTS AND DISCUSSION

Investigation of the uncatalyzed reaction identified four unique TSs corresponding to the chair and boat conformations with the phenyl group of the aldehyde either pseudoequatorial or pseudoaxial. The values of $\Delta G^{\ddagger}$ suggest the most favorable TS to be the chair conformation with the phenyl group equatorial (**TS-1$_{eq}$**, Figure 1). The corresponding axial TS is destabilized

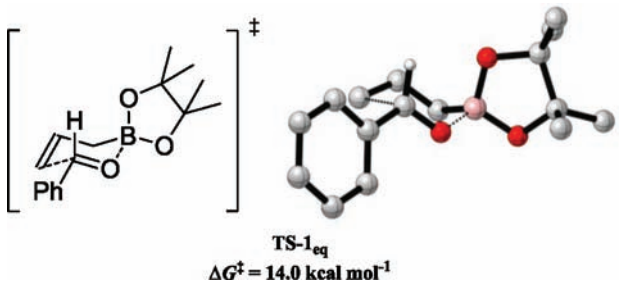

Figure 1. Preferred uncatalyzed transition structure. Geometry B3LYP/6-31G**, single-point energy M06-2X/6-31G**.

by steric interactions between the phenyl group of the aldehyde and the cyclic boronate (5.4 kcal mol^{-1} higher than **TS-1$_{eq}$**). Similarly, higher energies were observed for both boat TSs. Therefore, only **TS-1$_{eq}$** needs to be considered when examining the uncatalyzed pathway. The activation free energy of the uncatalyzed reaction was calculated to be 26.6 kcal mol^{-1} when evaluated using B3LYP/6-31G**. A similar study of the uncatalyzed reaction by Sakata et al. calculated $\Delta G^{\ddagger}$ to be 30.1 kcal mol^{-1} using B3LYP/6-311G** relative to the infinitely separated reagents.[3] When the Gibbs energy was corrected by taking a single-point energy using M06-2X/6-31G**, $\Delta G^{\ddagger}$ was lowered to 14.0 kcal mol^{-1}.

Investigation of the TS originally proposed by Antilla using buta-1,3-diene-1,4-diol-phosphoric acid as our simplest model catalyst reveals the value of $\Delta G^{\ddagger}$ to be 20.5 kcal mol^{-1} for **TS-2** when evaluated using B3LYP/6-31G** (Figure 2). This is significantly lower than the uncatalyzed activation barrier. It is possible, however, that there are even lower energy pathways.

Other possible modes of activation involve protonation of the carbonyl oxygen by the phosphoric acid (**TS-3**) and the formation of a 10-membered ring TS (**TS-4**). After the first reaction via **TS-4**, the catalyst would be regenerated as the boron-based species, which would lead to **TS-5**. However, all of these possibilities are disfavored relative to **TS-2**.

If the phosphoric acid hydrogen interacts with the pseudoaxial oxygen of the boronate, the phosphoryl oxygen can act as a Lewis basic site and establish a hydrogen bond to the formyl hydrogen. This stabilizing interaction provides rigidity in the transition state that could be responsible for the high levels of enantioselectivity observed (**TS-6**). **TS-6** is the lowest energy TS and also the tightest of the six-membered TSs with the shortest oxygen−hydrogen, carbon−carbon, and boron−oxygen distances (1.47, 2.11, and 1.50 Å, respectively). The formyl hydrogen bond has previously been identified as playing a crucial role in many asymmetric transformations.[24,25] Terada et al. also suggested that the formyl hydrogen bond was a key component in the BINOL-derived phosphoric acid-catalyzed enantioselective aza-ene-type reaction between glyoxylate and enecarbamate.[26] The lowest energy ground-state complex between aldehyde and catalyst was located, which involved both protonation of the oxygen of the aldehyde and an interaction from the phosphoryl oxygen of the catalyst to the formyl proton of the aldehyde.

Investigation of the potential energy surface using (*R*)-3,3′-bis(2,4,6-trimethylphenyl)-1,1′-bi-2-phenol as our second model catalyst suggested the lowest energy pathways to correspond to the six-membered TSs in which the phosphoric acid simultaneously interacts with the pseudoaxial oxygen of the boronate and with the formyl proton of the aldehyde through the Brønsted acid (proton) and Lewis basic (phosphoryl oxygen) sites, respectively (**TS-7*Re*** and **TS-7*Si***, Figure 3). In line with the buta-1,3-diene-1,4-diol-phosphoric acid model results, the 10-membered TSs were calculated to be less stable than the six-membered TSs (**TS-8*Re*** and **TS-8*Si***). Also, the free energy barrier for the catalyzed reaction through the most favorable *Re* six-membered TS reaction was ca. 6 kcal mol^{-1} lower than the barrier corresponding to the background reaction. The computed enantioselectivity arising from these calculations was found to be high and in agreement with the experimental value. We also located TSs similar to **TS-7*Re*** and **TS-7*Si***, which lack the interaction from the catalyst to the formyl proton (**TS-9*Re*** and **TS-9*Si***). These TSs involved single-point binding from the catalyst to the substrate, like Antilla's proposed mode of activation, and were higher in energy than **TS-7*Re*** and **TS-7*Si***.

Comparison of **TS-7*Si*** and **TS-9*Si*** provided an estimate of the strength of the formyl hydrogen bond. Superposition of the allylboronic acid pinacol ester and benzaldehyde from both TSs leads to an rmsd of 0.0568 between the two structures. This suggests that the primary reason for a difference in energy can be attributed to the formyl hydrogen bond. The difference in free energy was found to be 2.7 kcal mol^{-1}, in close agreement with the strength suggested by Weber et al., who estimated the average strength of the formyl hydrogen bond falls in the range of 2.4−3.6 kcal mol^{-1}.[27]

dx.doi.org/10.1021/ja210200d | *J. Am. Chem.Soc.* 2012, 134, 2716−2722

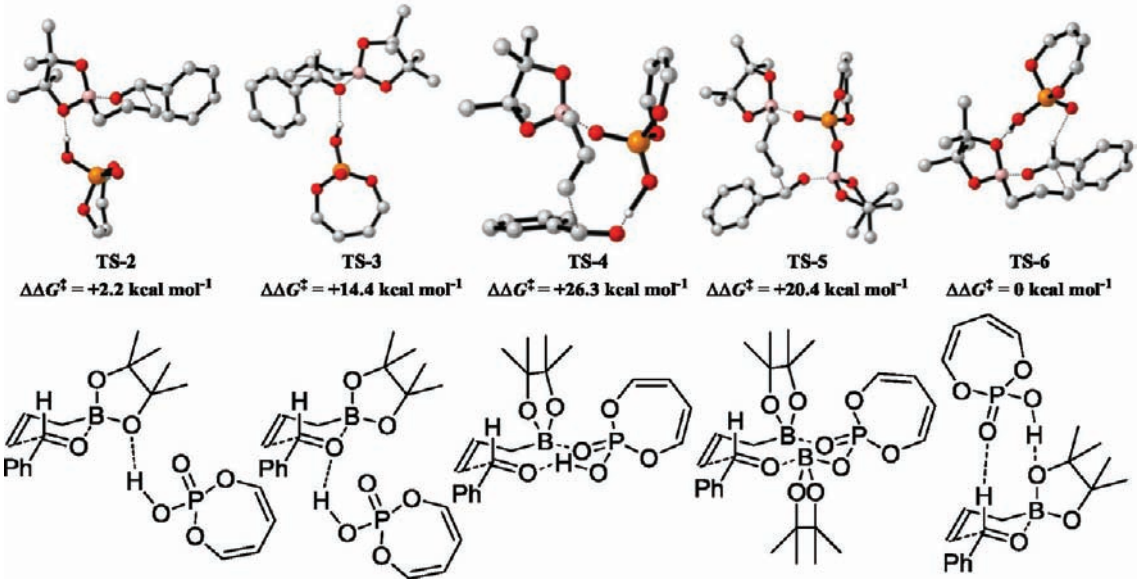

Figure 2. Competing transition structures for the reaction of benzaldehyde catalyzed by buta-1,3-diene-1,4-diol-phosphoric acid. Geometry B3LYP/6-31G**, single-point energy M06-2X/6-31G**.

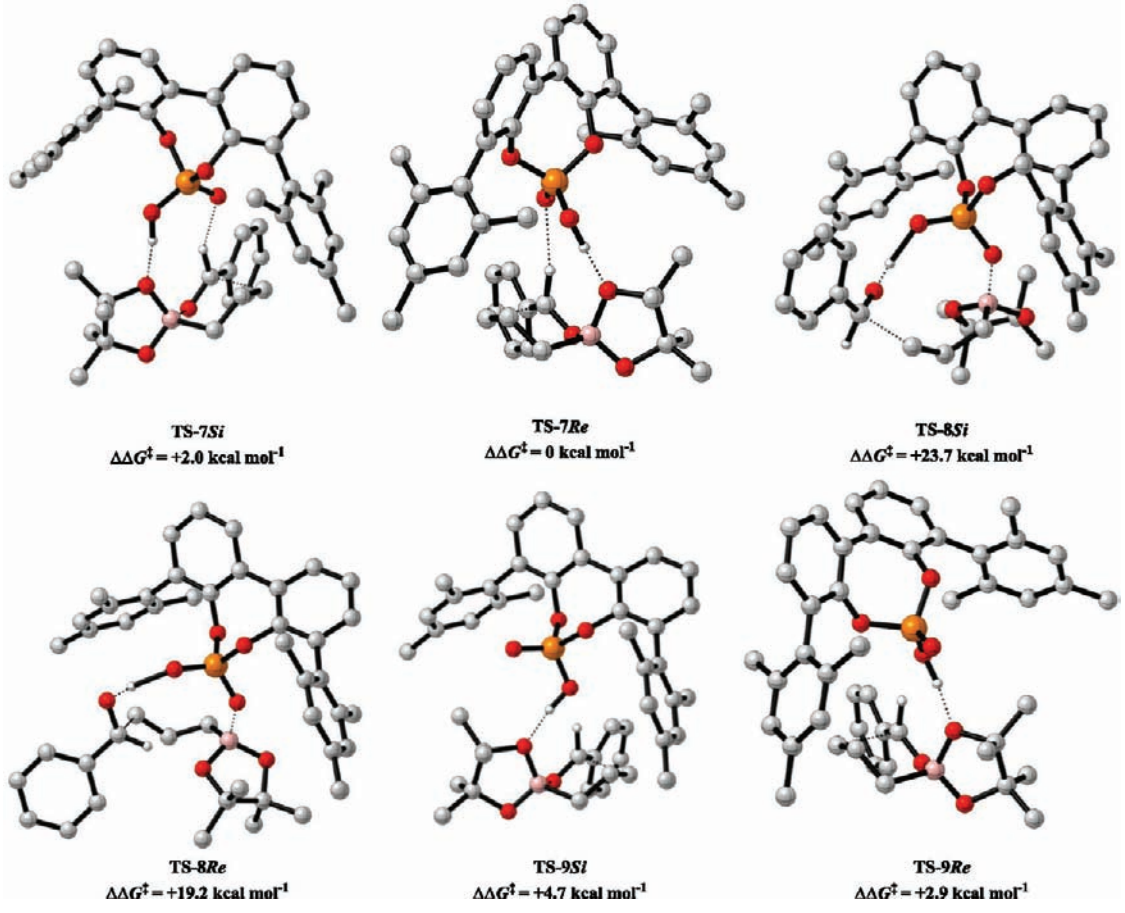

Figure 3. Competing transition structures for the reaction of benzaldehyde using the (*R*)-3,3′-bis(2,4,6-trimethylphenyl)-1,1′-bi-2-phenol model system. Optimized transition structure geometries B3LYP/6-31G*.

Transition states for the full catalyst were located using ONIOM for several of the possible reaction pathways, and these confirmed that the same trends in activation energies were present as for the model catalyst systems. These results show that ONIOM calculations are effective for this system.

The 10-membered ring TSs (**TS-10** and **TS-11**, Figure 4) were strongly disfavored relative to the six-membered ring TSs, a result expected on the basis of the outcome of the model studies. For Antilla's proposed mode of activation, 24 unique transition structures were located due to the conformational

dx.doi.org/10.1021/ja210200d | *J. Am. Chem.Soc.* 2012, 134, 2716–2722

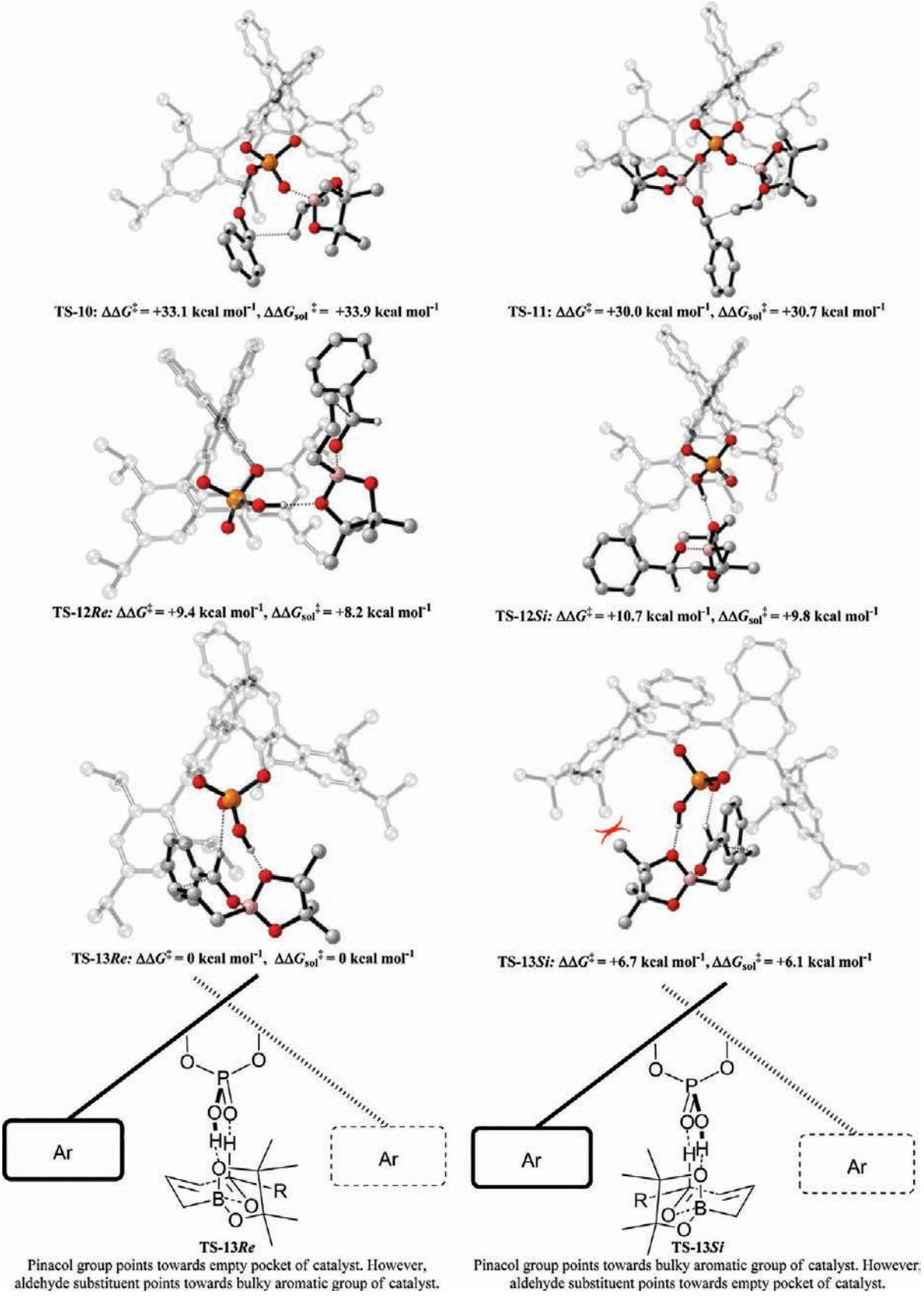

Figure 4. Competing transition states for the reaction of benzaldehyde. ONIOM(B3LYP/6-31G**:UFF), single-point energy M06-2X/6-31G**. Grayed-out regions were treated with UFF, and the full-color regions were treated with B3LYP/6-31G**.

flexibility associated with rotation about the single hydrogen-bonding interaction to the substrate. Of these TSs, **TS-12*Re*** and ***Si*** were the lowest energy structures. **TS-12*Si*** was found to be disfavored relative to **TS-12*Re*** by 1.3 kcal mol^{-1}.

dx.doi.org/10.1021/ja210200d | *J. Am. Chem.Soc.* 2012, 134, 2716–2722

However, **TS-13*Re*** was found to be the most favorable and also the tightest of the six-membered TSs with the shortest oxygen−hydrogen, carbon−carbon, and boron−oxygen distances, consistent with the findings of the buta-1,3-diene-1,4-diol-phosphoric acid model study (Figure 4 and Table 1).

Table 1. Interatomic Distances for Key ONIOM TSs

	interatomic distance (Å)			
	O−H (boronate protonation)	C−C	B−O	CH−O (formyl hydrogen)
TS-12*Re*	1.59	2.21	1.51	
TS-12*Si*	1.62	2.22	1.52	
TS-13*Si*	1.59	2.13	1.50	2.19
TS-13*Re*	1.45	2.09	1.49	2.15

TS-13*Re* is favored over **TS-13*Si*** by 6.7 kcal mol^{-1}. Using the calculated Boltzmann ratios of both TSs at 243 K, the expected enantiomeric excess (ee) from this pathway is >99.9% in close agreement with the observed experimental outcome. Reasons for such strong selectivity toward the (*R*)-homoallylic alcohol originate from the unfavorable steric clash between the pinacol ester methyl groups and the large aromatic group of the catalyst, which disfavors **TS-13*Si*** relative to **TS-13*Re***. Because of the concerted and apolar nature of the transition structures, solvent effects were shown to have minimal effect on the values of $\Delta\Delta G_{sol}^{\ddagger}$ (Figure 4).

Although the activation modes of **TS-13** and Antilla's proposed TS (**TS-12**) are similar, the former is substantially more energetically preferable. To rationalize this, TSs were located for the latter activation mode in conformations that closely resembled that of **TS-13*Re*** and **TS-13*Si***, but lacked a phosphoryl oxygen−formyl proton interaction (**TS-14*Re*** and **TS-14*Si***, Figure 5). These TSs were disfavored relative to **TS-13*Re*** and **TS-13*Si***. Approximately 2.7 kcal mol^{-1} of the energy difference can be attributed to the absence of the formyl hydrogen bond. **TS-14*Re*** is destabilized relative to **TS-13*Re*** because the pinacol group must

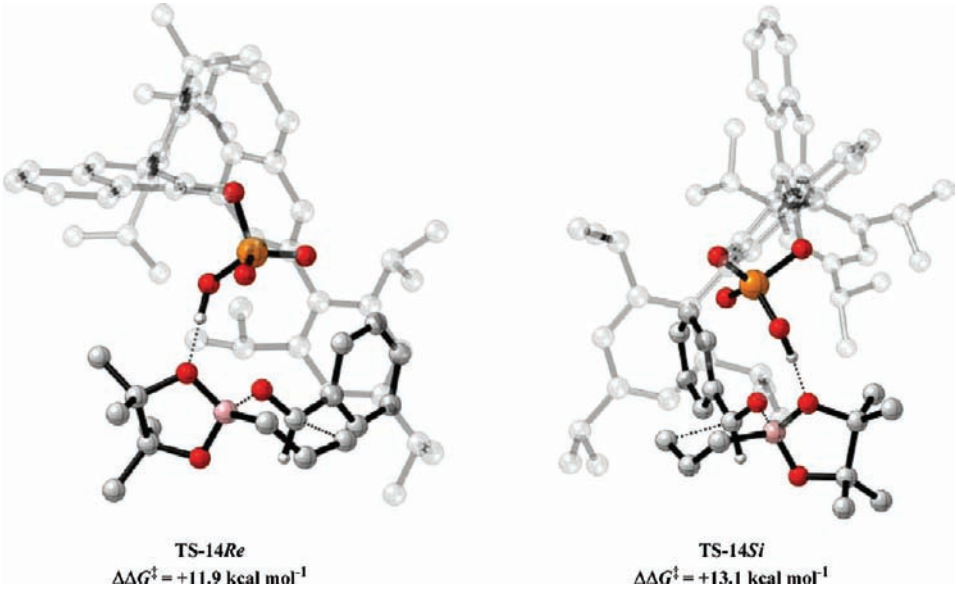

Figure 5. Optimized transition structure geometries for the reaction of benzaldehyde. ONIOM(B3LYP/6-31G**:UFF), single-point energy M06-2X/6-31G**. Grayed-out regions were treated with UFF, and the full-color regions were treated with B3LYP/6-31G**.

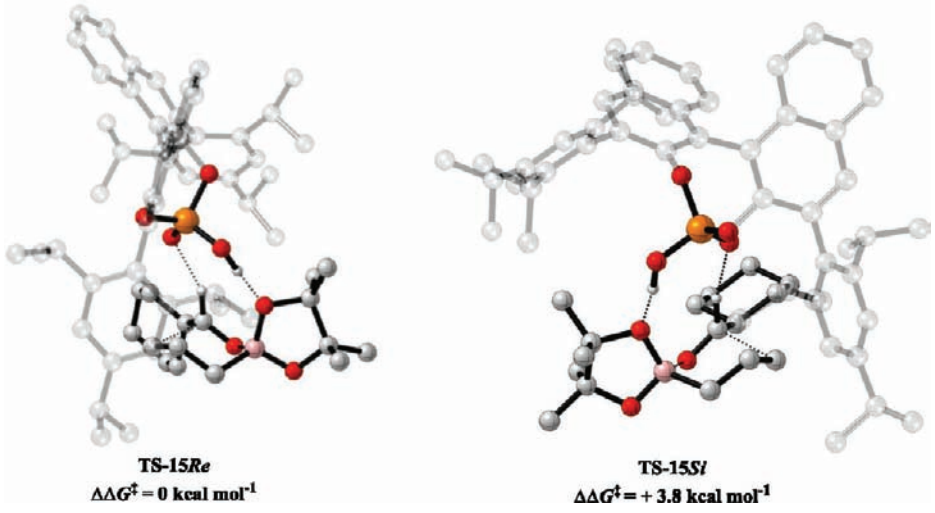

Figure 6. Optimized transition structure geometries for the reaction of cyclohexanecarbaldehyde. ONIOM(B3LYP/6-31G**:UFF), single-point energy M06-2X/6-31G**. Grayed-out regions were treated with UFF, and the full-color regions were treated with B3LYP/6-31G**.

dx.doi.org/10.1021/ja210200d | *J. Am. Chem.Soc.* 2012, 134, 2716−2722

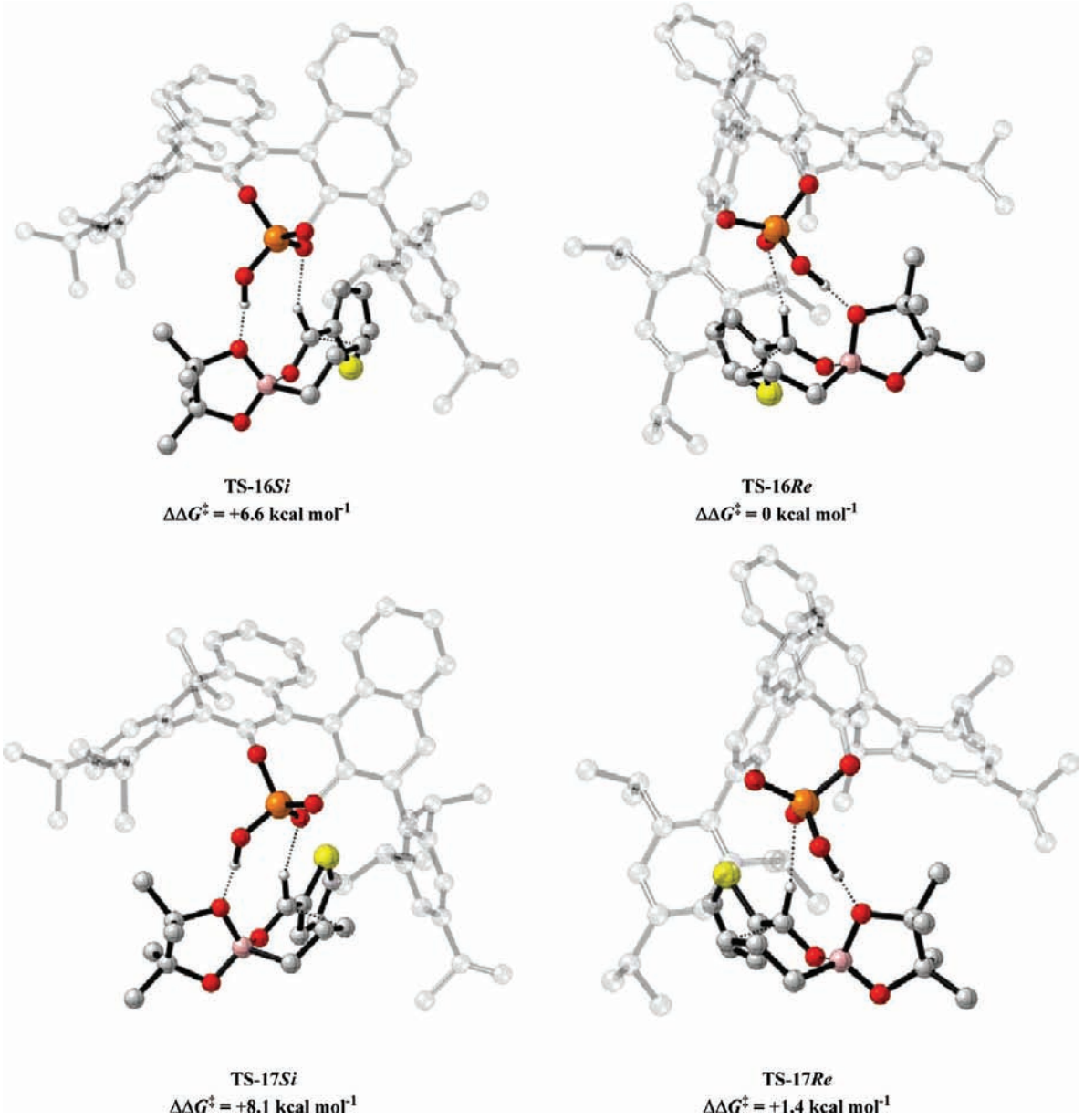

Figure 7. Competing transition structures for the reaction of thiophene-2-carbaldehyde. ONIOM(B3LYP/6-31G**:UFF), single-point energy M06-2X/6-31G**. Grayed-out regions were treated with UFF, and the full-color regions were treated with B3LYP/6-31G**.

now be orientated toward the bulky pocket of the catalyst. **TS-14*Si*** places the pinacol group in the empty pocket of the catalyst but is destabilized relative to **TS-13*Si*** because the aldehyde substituent must now be accommodated in the sterically demanding pocket of the catalyst. Because of the flexible nature of this monocoordination activation mode, lower energy TSs (**TS-12*Re*** and **TS-12*Si***) were located, which avoid these unfavorable steric interactions. However, the strength of the hydrogen bond to the cyclic boronate is compromised in these sterically more accessible conformations. The angle of the hydrogen bond deviates away from near linear (178°) in the case of **TS-14*Re*** to 164° in **TS-12*Re*** and lengthens from 1.56 to 1.59 Å. In the case of **TS-12*Si***, the linear hydrogen-bonding arrangement is present, but the length of this interaction was found to be longer in **TS-12*Si*** (1.62 Å) than in **TS-14*Si*** (1.53 Å). Therefore, the reason for the large energetic preference for **TS-13*Re*** and **TS-13*Si*** is a combination of both steric and electronic factors as well as the presence of the formyl hydrogen bond.

The biphenol derived model system indicates that the energy difference between **TS-13*Re*** and **TS-13*Si*** is overestimated by the ONIOM method. This is due to the UFF component of the optimization, which overestimates short-range repulsion effects.[28] Although the absolute values are larger as compared to our DFT optimized structures, the method still accurately predicts changes in levels of enantioselectivity. The lowest experimentally observed enantioselectivity was 73% in the case of cyclohexanecarbaldehyde. **TS-15*Re*** and **TS-15*Si*** (Figure 6) were located, and the energy difference (3.8 kcal mol^{-1}) was found to be significantly lower than for the corresponding TSs involving benzaldehyde (6.7 kcal mol^{-1}). While the energy difference is still overestimated, the reproduction of experimental enantioselectivity trends illustrates the strength of the formyl proton hydrogen-bonded transition state model. Therefore, the model can be used to predict approximate enantioselectivities of novel aldehydes, relative to benzaldehyde.

dx.doi.org/10.1021/ja210200d | *J. Am. Chem.Soc.* 2012, 134, 2716–2722

Although the clash of the pinacol ester methyl groups with the catalyst's bulky aromatic substituent controls the absolute stereochemistry, the aldehyde substituent can destabilize the *Re* relative to the *Si* TS. This is due to minimization of the unfavorable pinacol interaction with the catalyst increasing the aldehyde clash. The pinacol group fits into the empty pocket of the catalyst; however, this means that the aldehyde substituent must be accommodated in the sterically demanding pocket (Figure 4, R = cyclohexyl). The cyclohexane ring clashes with the catalyst more strongly than in the case of the flat phenyl group of benzaldehyde. This stabilizes *Si* relative to *Re*, but the overriding effect is still the clash of the pinacol group and the preference for *Re*-face attack is maintained.

Experimental Test of the Model. Antilla's results suggest *Re*-face attack in every example except for attack on thiophene-2-carbaldehyde. (2-(Benzyloxy)acetaldehyde was reported to yield the (*S*)-enantiomer, corresponding to *Si*-face attack, by analysis of the optical rotation. However, after reviewing the Supporting Information, the data suggest that the *R* product is formed.[29]) This leads to the *R* product in most cases. For 3-phenylpropanal, the low priority of the unbranched side chain results in the *S* product from *Re*-face attack. In the case of thiophene-2-carbaldehyde, our calculations suggest that *Re*-face attack should also be expected. ONIOM calculations were performed in the same manner as those reported for the reaction of benzaldehyde. According to our calculations, **TS-16*Re*** is favored over **TS-16*Si*** by 6.6 kcal mol^{-1}, a value very similar to that calculated for the reaction of benzaldehyde (Figure 7). The orientation of the thiophene moiety was found to be important with **TS-17*Re*** and **TS-17*Si*** disfavored by approximately 1.4 kcal mol^{-1} relative to **TS-16*Re*** and **TS-16*Si***, respectively.

Therefore, to test our mechanistic hypothesis, the reaction of allylboronic acid pinacol ester and thiophene-2-carbaldehyde was repeated under the same conditions as described by Antilla (see the Supporting Information). Chiral HPLC analysis indicated that the ee generated by the reaction was 96%. The product displayed the opposite sense of optical rotation to that reported in the original paper. The absolute stereochemistry of the product was determined by analysis of both diastereomeric Mosher esters (see the Supporting Information). The results indicated that the product formed was the (*R*)-homoallylic alcohol, in full agreement with our calculations.

4. CONCLUDING REMARKS

DFT and QM/MM hybrid calculations suggest that the phosphoric acid-catalyzed allylboration of aldehydes involves a highly ordered transition structure in which there is a hydrogen-bonding interaction from the catalyst hydroxyl group to the pseudoaxial oxygen of the cyclic boronate. An additional stabilizing interaction from the phosphoryl oxygen of the catalyst to the formyl hydrogen of the aldehyde lowers the energy of the transition state and provides extra rigidity to the system. This transition structure is lower in energy than the one proposed in the original paper.[9] The role of the formyl hydrogen bond as a key element that controls the enantioselectivity of a reaction catalyzed by a BINOL-derived phosphoric acid proposed herein should promote future developments in the field. Our calculations suggest a qualitative model (Figure 4) that accurately reproduces the experimentally observed enantioselectivity in all cases. The model highlights and leads to the correction of a misassignment of absolute configuration in the original data.

■ ASSOCIATED CONTENT

Supporting Information

Complete list of authors in the Gaussian 03 reference; Cartesian coordinates, energies, and number of imaginary frequencies of all stationary points and values of imaginary frequencies of all transition structures; and full experimental details. This material is available free of charge via the Internet at http://pubs.acs.org.

■ AUTHOR INFORMATION

Corresponding Author

jmg11@cam.ac.uk

■ ACKNOWLEDGMENTS

M.N.G. and J.M.G. thank the EPSRC for funding and Unilever. S.C.P. thanks CONICET, UNR, and ANPCyT.

■ REFERENCES

(1) Yamamoto, Y.; Asao, N. *Chem. Rev.* **1993**, *93*, 2207.
(2) Denmark, S. E.; Fu, J. *Chem. Rev.* **2003**, *103*, 2763.
(3) Sakata, K.; Fujimoto, H. *J. Am. Chem. Soc.* **2008**, *130*, 12519.
(4) Li, Y.; Houk, K. N. *J. Am. Chem. Soc.* **1989**, *111*, 1236.
(5) Brown, H. C.; Jadhav, P. K. *J. Am. Chem. Soc.* **1983**, *105*, 2092.
(6) Brown, H. C.; Bhat, K. S. *J. Am. Chem. Soc.* **1986**, *108*, 293.
(7) Rauniyar, V.; Hall, D. G. *J. Org. Chem.* **2009**, *74*, 4236.
(8) Wada, R.; Oisaki, K.; Kanai, M.; Shibasaki, M. *J. Am. Chem. Soc.* **2004**, *126*, 8910.
(9) Jain, P.; Antilla, J. C. *J. Am. Chem. Soc.* **2010**, *132*, 11884.
(10) Simón, L.; Goodman, J. M. *J. Am. Chem. Soc.* **2008**, *130*, 8741.
(11) Simón, L.; Goodman, J. M. *J. Am. Chem. Soc.* **2009**, *131*, 4070.
(12) *Jaguar*, version 7.6; Schrodinger, LLC: New York, 2009.
(13) Becke, A. D. *Phys. Rev. A* **1988**, *38*, 3098.
(14) Lee, C.; Yang, W.; Parr, R. G. *Phys. Rev. B* **1988**, *37*, 785.
(15) Krishnan, R.; Binkley, J. S.; Seeger, R.; Pople, J. A. *J. Chem. Phys.* **1980**, *72*, 650.
(16) Gill, P. M. W.; Johnson, B. G.; Pople, J. A.; Frisch, M. J. *Chem. Phys. Lett.* **1992**, *197*, 499.
(17) Zhao, Y.; Truhlar, D. *Theor. Chem. Acc.* **2008**, *120*, 215.
(18) Simón, L.; Goodman, J. M. *Org. Biomol. Chem.* **2011**, *9*, 689.
(19) Yamanaka, M.; Hirata, T. *J. Org. Chem.* **2009**, *74*, 3266.
(20) Frisch, M. J.; et al. *Gaussian 03*; Gaussian, Inc.: Wallingford, CT, 2004.
(21) Rappe, A. K.; Casewit, C. J.; Colwell, K. S.; Goddard, W. A.; Skiff, W. M. *J. Am. Chem. Soc.* **1992**, *114*, 10024.
(22) Simón, L.; Goodman, J. M. *J. Org. Chem.* **2010**, *75*, 589.
(23) Mennucci, B.; Tomasi, J. *J. Chem. Phys.* **1997**, *106*, 5151.
(24) Corey, E. J.; Lee, T. W. *Chem. Commun.* **2001**, 1321.
(25) Paton, R. S.; Goodman, J. M. *J. Org. Chem.* **2008**, *73*, 1253.
(26) Terada, M.; Soga, K.; Momiyama, N. *Angew. Chem., Int. Ed.* **2008**, *47*, 4122.
(27) Neuheuser, T.; Hess, B. A.; Reutel, C.; Weber, E. *J. Phys. Chem.* **1994**, *98*, 6459.
(28) Zgarbova, M.; Otyepka, M.; Sponer, J.; Hobza, P.; Jurecka, P. *Phys. Chem. Chem. Phys.* **2010**, *12*, 10476.
(29) Lee, J.-Y.; Miller, J. J.; Hamilton, S. S.; Sigman, M. S. *Org. Lett.* **2005**, *7*, 1837.